THE JOURNAL OF COMPARATIVE NEUROLOGY 398:225–240 (1998)

Critical Assessment of the Involvement of Perforations, Spinules, and Spine Branching in Hippocampal Synapse Formation

KARIN E. SORRA,[1,2] JOHN C. FIALA,[2] AND KRISTEN M. HARRIS[1,2]*
[1]Program in Neuroscience, Harvard Medical School, Boston, Massachusetts 02115
[2]Division of Neuroscience in the Department of Neurology, Children's Hospital, Boston, Massachusetts 02115

ABSTRACT

Several studies propose that long-term enhancement of synaptic transmission between neurons results from the enlargement, perforation, and splitting of synapses and dendritic spines. Unbiased analyses through serial electron microscopy were used to assess the morphological basis for synapse splitting in hippocampal area CA1. Few perforated synapses and almost no split (i.e., branched) spines occurred at postnatal day 15, an age of high synaptogenesis; thus, synapse splitting is unlikely to be important during development. The synapse splitting hypothesis predicts an intermediate stage of branched spines with both heads sharing the same presynaptic bouton. Ninety-one branched dendritic spines were traced through serial sections, and the different branches never synapsed with the same presynaptic bouton. Projections from spines, called "spinules," have been thought to extend from perforations in the postsynaptic density (PSD), thereby dividing the presynaptic bouton. Forty-six spinules were traced, and only 13% emerged from perforations in the PSD. Most spinules emerged from the edges of nonperforated PSDs, or from spine necks, where they extended into boutons that were not presynaptic to the spine. In summary, these morphological characteristics are inconsistent with synapse and spine splitting. An alternative is discussed whereby perforated synapses and spinules are transient components of synaptic activation, and branched spines appear from synapses forming in close proximity to one another. J. Comp. Neurol. 398:225–240, 1998.

Indexing terms: serial electron microscopy; postsynaptic density; three-dimensional reconstructions; synaptogenesis; plasticity; hippocampal slices

Dendritic spines are the principal postsynaptic targets of excitatory synapses in the central nervous system. The excitatory synapses occur on the swollen heads of dendritic spines that are long or short, fat or thin, branched or unbranched (Harris and Kater, 1994). Dendritic spines are the subject of many studies which illustrate a dramatic variation and plasticity in spine number and structure, even in the mature central nervous system (Horner, 1993; Jones and Harris, 1995; Papa and Segal, 1996; Woolley et al., 1996). Nevertheless, many basic questions about the structure and function of spines remain.

One important question is: How are new dendritic spines formed? Recent studies of hippocampal development suggest dendritic filopodia attract axons to the dendrite (Dailey and Smith, 1996), and eventually give rise to spines of varying morphologies (Harris et al., 1992). A prevalent model for how new spines form in the mature brain suggests that existing spines and synapses "split," thereby giving rise to two or more daughter synapses (Nieto-Sampedro et al., 1982; Carlin and Siekevitz, 1983; Dyson and Jones, 1984; Geinisman et al., 1993, 1996; Jones and Harris, 1995; Edwards, 1995; Bolshakov et al., 1997). Key features of how synapses and spines could split

Grant sponsor: NIH; Grant numbers: NS21184, NS33574; Grant sponsors: NIMH, NIDA, NASA; Grant number: MH/DA57351; Grant sponsor: NIH; Grant number: P30-HD18655; Grant sponsor: Harvard Medical School; Grant sponsor: Natural Sciences and Engineering Research Council of Canada.

*Correspondence to: Kristen M. Harris, Ph.D., Division of Neuroscience, Enders 260, Children's Hospital, 300 Longwood Ave., Boston, MA 02115. E-mail: harrisk@hub.tch.harvard.edu

Received 11 December 1997; Revised 17 April 1998; Accepted 19 April 1998

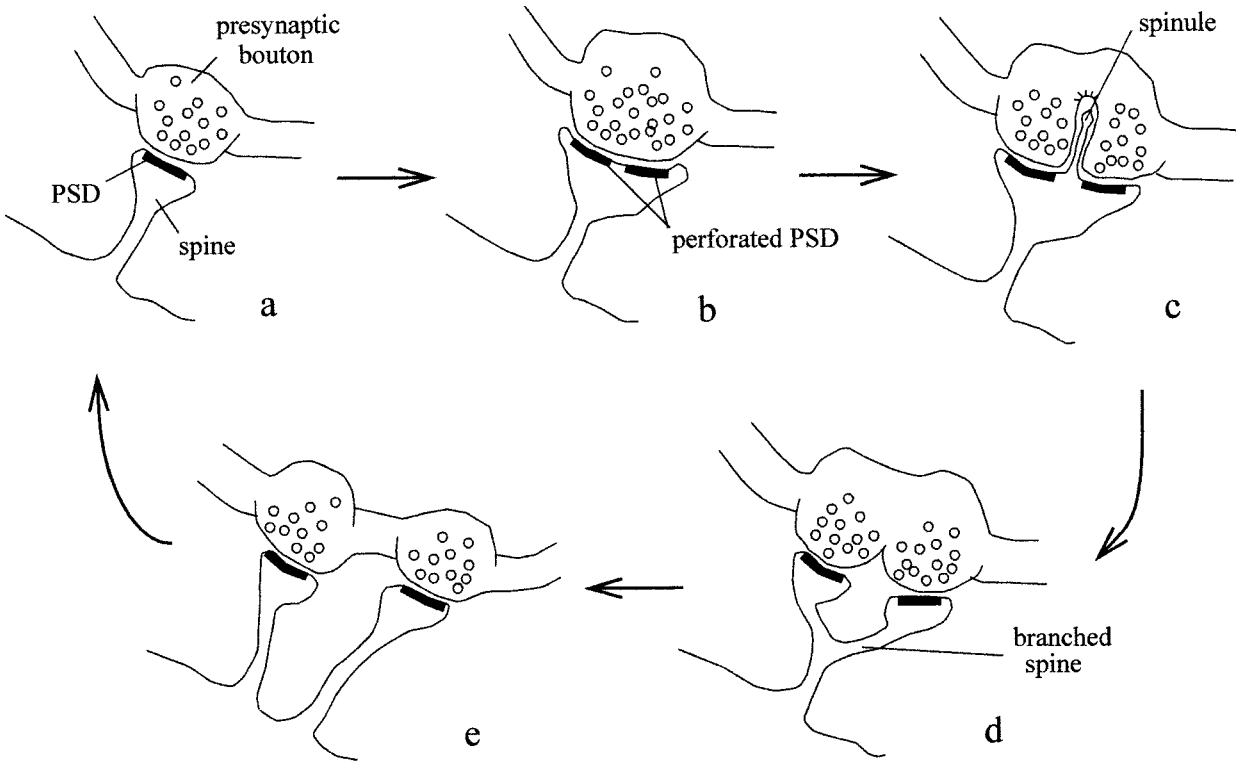

Fig. 1. Model of synapse splitting. **a:** Start with a spine having a macular synapse. **b:** A perforation forms in the macular synapse. **c:** A synaptic spinule extends from a gap in the perforation into the presynaptic bouton dividing the presynaptic terminal into separate synaptic compartments. **d:** The spinule retracts and the spine begins to split, creating a branched spine with both heads sharing a single presynaptic bouton. **e:** Complete splitting results in the formation of two daughter spines, although their boutons would still originate from the same axon. PSD, postsynaptic density.

are depicted in Figure 1. First, the postsynaptic density (PSD) of small synapses (Fig. 1a) enlarges and perforates (Fig. 1b). A concomitant division of the presynaptic bouton is achieved by spinules projecting from the perforation in the dividing PSD into the presynaptic bouton (Fig. 1c). As the synapse splits further, the spinule is retracted. At some stage during synapse splitting, a branched dendritic spine occurs with at least two heads synapsing with the same presynaptic axon (Fig. 1d). Subsequently, daughter dendritic spines are generated from each segment of the previously perforated synapse (Fig. 1e).

Branched dendritic spines are relatively rare, comprising less than 10% of all synapses in a brain region (Harris and Stevens, 1988; Chicurel and Harris, 1992; Trommald and Hulleberg, 1997). There is evidence for an increase in the frequency of branched spines in the adult central nervous system (CNS) under varying degrees of synaptic plasticity including chronic exposure to amphetamines (Robinson and Kolb, 1997), rearing in an enriched environment (Jones et al., 1997), long-term potentiation (LTP) in hippocampal area dentata (Trommald et al., 1990); however, not with LTP in hippocampal area CA1 (Sorra and Harris, 1998). Overall, the findings suggest that the frequency of branched dendritic spines increases when there are more synapses.

Spinules were first described in area CA1 as small narrow projections of the dendritic surface (Westrum and Blackstad, 1962). They usually originate from the head or neck of a spine, often near to, but never directly from the postsynaptic density. Spinules have been observed projecting into boutons, but not necessarily into the boutons that were presynaptic to the spines from which they originated. Spinules have been observed at axospinous synapses in many different brain regions (Tarrant and Routtenberg, 1977; Spacek, 1985), and the frequency of synaptic spinules increases with synaptic activation and plasticity (Applegate and Landfield, 1988; Schuster et al., 1990), but their role in synapse proliferation remains controversial.

Recently, synapse splitting has been proposed as one mechanism whereby new synapses might be formed during the late phase of LTP (occurring after 1–2 hours) in hippocampal area CA1 (Bolshakov et al., 1997). Synapse number is stable at 2 hours after LTP in hippocampal area CA1 (Sorra and Harris, 1998); however, it is not known whether synapse number changes at earlier or later times after induction of LTP. In contrast, the reverse of the splitting cycle has been proposed to account for spine loss during LTP in hippocampal area dentata, via fusion of neighboring spines into branched spines (Rusakov et al., 1997). These results contrast with other findings in area dentata, in which synapse proliferation is associated with an increase in branched spines after LTP (Trommald et al., 1990). Even though there is controversy regarding changes in synapse number as a basis for functional synaptic plasticity, the validity of the synapse-splitting hypothesis can be tested directly, because it requires the occurrence of the various structural intermediates. In this study, serial electron microscopy was used to assess whether the needed

structural intermediates of the synapse splitting hypothesis occur in hippocampal area CA1.

MATERIALS AND METHODS

Tissue preparation

Serial electron micrographs of perfusion-fixed hippocampus were available from male rats of the Long-Evans strain aged 15 days postnatal (n = 2), and 40 and 77 days postnatal (n = 2, referred to as "adult" in this paper, although technically they are young adults; Harris and Stevens, 1989; Harris et al., 1992) and from adult hippocampal slices (Sorra and Harris, 1998). All of our procedures follow NIH guidelines and undergo yearly review by the Animal Care and Use Committee at Children's Hospital.

For the perfusion-fixed hippocampus, intracardiac perfusions were performed under deep pentobarbital anesthesia (80 mg/Kg), with fixative containing 2% paraformaldehyde, 2.5% glutaraldehyde, and 2 mM $CaCl_2$ in 0.1 M cacodylate buffer at pH 7.35, 37°C, and 4 psi backing pressure from compressed gas (95% O_2, 5% CO_2). One hour after perfusion, the hippocampi were dissected and then sliced at 400 μm and washed with slow continuous agitation in five changes of buffer over 30–45 minutes, soaked for 1 hour in 1% OsO_4 with 1.5% $K_4Fe(CN)_6$, for 1 hour in OsO_4, then rinsed five times over 30 minutes in buffer and two quick changes of water. The 400-μm slices were then dehydrated through graded ethanols, including 1% uranyl acetate in 70% ethanol for 1 hour, up to 100% ethanol (four changes for 10 minutes each). Two short rinses with propylene oxide were followed by embedding in Epon (equal proportions of Epon and propylene oxide overnight, and then Epon at 60°C for 48 hours). Warm Epon blocks (60°C) were first hand-trimmed with a razor blade and then precision-trimmed with the corner of a glass knife at room temperature on a Reichert Ultracut III ultramicrotome to a thin trapezoid containing the CA1 pyramidal cell bodies and the entire apical dendritic arbor. Serial sections were mounted on Formvar-coated slot grids, stained with Reynolds' lead citrate, and stored in grid cassettes for photography at a JEOL 100B electron microscope (initial magnifications of ×6,600 or 15,000). Four electron microscopic (EM) series from the postnatal day (P)15 animals (35–39 sections per series), 5 series from the young adult perfused tissue (27–68 sections per series) were analyzed.

Hippocampal slices were prepared from male Long-Evans rats aged 60–70 days (236–310 g; Sorra and Harris, 1998). After equilibrating for 1 hour in vitro, control slices were maintained for 1–13 hours in vitro and subjected to electrophysiological analysis of extracellular field potentials to assess slice health and excitability (Sorra and Harris, 1998). Increasing stimulus intensity was used to generate an input-output (I-O) curve and the half-maximal responses were monitored for 20–40 minutes to ensure response stability just prior to fixation. Adjacent slices were subjected to a tetanic stimulation protocol, resulting in LTP. Representative physiological recordings from the hippocampal slices are published in Sorra and Harris (1998).

Immediately following the physiological recordings, slices were fixed for 8–10 seconds in mixed aldehydes (6% glutaraldehyde, 2% paraformaldehyde, 2 mM $CaCl_2$, 4 mM $MgSO_4$ in 0.1 M cacodylate buffer at pH 7.4) using a 700 watt Amana microwave oven (Jensen and Harris, 1989). The slices were then processed for serial EM as described above, except they were mounted on Pioloform-coated slot grids and photographed at a JEOL 1200EX electron microscope (initial magnification 6,000×). Ten series (27–58 sections per series) were examined from the middle of stratum radiatum in these hippocampal slices. Only data from the control slices were used for quantitative comparisons of synapse densities across ages. LTP slices were only used to evaluate the morphological diversity in branched spines. We have already reported that the frequency of branched spines does not change with LTP in area CA1 (Sorra and Harris, 1998). Here, we found the full range in morphological diversity of branched spines in both the control and LTP slices; hence, they are included in the total adult population of Table 1 as described in the Results section.

Unbiased analysis of synapse frequencies using the volume disector

The volume disector was elaborated from the series sample method used in Harris et al. (1992) to obtain unbiased estimates of synapse densities and relative percentages (Figs. 3–5). The volume disector has three steps. First, a sample area is defined in which all of the synapses are accurately identified by viewing them through adjacent serial EMs. Second, an adjusted area of the sampling field, the homogeneous neuropil area (HNA) is determined. Finally, the density of synapses is adjusted for variation in section thickness and viewing probability based on the size, shape, or orientation of the synapse. Thus, the volume disector is based on many of the same principles as the physical disector (Braengaard and Gundersen, 1986; Coggeshall and Lekan, 1996). The main advantage of the volume disector is that all of the synapses viewed through serial sections are retained in the final sample, not just those that disappear between a pair of sections, as in the physical disector. All synapses can be retained because the probability of viewing each synapse is corrected empirically by computing the number of sections it occupies. The volume disector was especially useful for analyzing branched dendritic spines, which occur so infrequently in the relatively small samples of the neuropil that can be analyzed, as discussed in the Results section.

To define the sample area, a rectangular sampling frame was drawn on the cover sheet of a middle reference section. Two sides of the rectangle were randomly assigned as inclusion edges, and the remaining two sides were exclusion edges, as in the two-dimensional counting frame of Gundersen (1978). PSDs occurring within the sample frame or on the inclusion lines were counted, and those occurring outside of the frame or on the exclusion lines were not counted. Synapses within the sample field were counted if the PSD and synaptic vesicles occurred on the reference section. PSDs sectioned en face were included if the synaptic vesicles appeared in the immediately adjacent section.

To compute the HNA, the cross-sectional areas occupied by large objects which occur nonuniformly across different samples (including portions of dendrites, cell bodies, blood vessels, glia etc., having an area greater than 1 μm^2, Harris et al., 1989) were subtracted from the sampling area. The sampling frame from each series was digitized by using a CCD camera interfaced to the Vision-8 PC-based frame grabber (Insync Technologies, San Leandro, (CA). The sample frames and large nonuniform objects

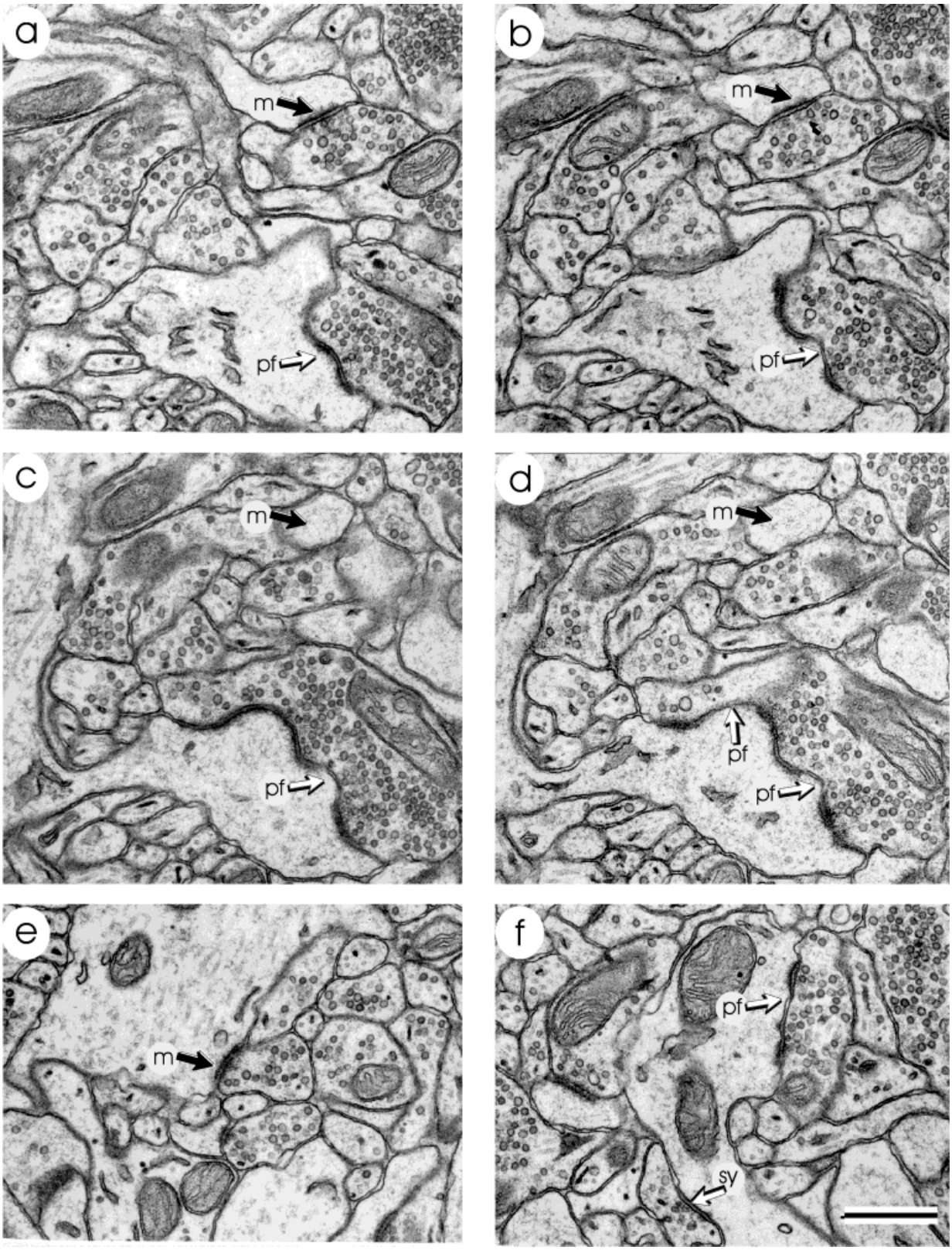

Fig. 2. Macular and perforated synapses in perfusion-fixed neuropil in area CA1 of the adult hippocampus. Partial set of serial sections through macular and perforated synapses on unbranched dendritic spines. A macular synapse (m) is identified in a and b on the head of a thin spine which is also labelled m in c and d, although the PSD is not present in those two sections. **a–d:** A perforated synapse (pf) is identified on the head of a mushroom spine and the arrow is directed to where the perforation occurs in b and c; and in d a second perforation occurs at the left side of the synapse. **e:** Macular synapse (m) on the shaft of a spiny dendrite. **f:** Perforated synapse (pf) on the shaft of a spiny dendrite. A symmetric shaft synapse (sy) also occurs on this dendrite. This type of synapse was not included in the quantitative analysis because they are likely to be inhibitory and not involved in spine branching (Peters et al., 1991). Dendrites were confirmed as spiny by the presence of spines originating from them when viewed through serial sections. The nonspiny dendrites of interneurons were not included. Scale bar = 0.5 μm.

were traced and their areas were computed by using software entitled *V8* developed in the Children's Hospital Image Graphics Laboratory (IGL).

Thicker sections contain more synaptic profiles than thinner sections; hence, section thickness was estimated for each series. To compute section thickness, the diameters of longitudinally sectioned mitochondria were measured in single sections. Then, the number of serial sections occupied by each mitochondrion was counted at the exact point where the diameter was measured. Because mitochondria are cylindrical in shape, section thickness was computed as: thickness (μm/section) = measured diameter/number of sections spanned by the mitochondrion. The mean section thickness for each series was obtained by measuring 5 to 20 longitudinally oriented mitochondria (see also Harris and Stevens, 1988, 1989; Harris et al., 1992).

Variation in the probability of viewing PSDs can be simultaneously corrected for size, shape, and orientation with respect to the plane of section because each of these factors influences proportionally the number of sections the PSD occupies in a series. For each PSD identified on a reference section, the number of serial sections it occupied was counted. When grouping the synapses by PSD morphology or spine shape, the number of sections for the PSDs in each category of identification was averaged.

The following formula was used to obtain synapse densities appropriately corrected for differences in HNA, probability of viewing synapses of different shapes and sizes, and for differences in section thickness: adjusted synapse density (ASD, number per 100 μm^3) = (number of synapses $\times$ 100)/HNA $*$ (1/mean section thickness) $*$ (1/mean no. of sections per PSD). To compute the relative percentages of different types of synapses, the ASD of a particular type of synapse was divided by the ASD of total synapses and multiplied by 100.

Analysis of spinules

Five EM series (1 from perfusion-fixed hippocampus and 4 from the slice experiments) were used for an analysis of spinule locations. Synaptic spinules are thin projections of cytoplasm and membrane of the spine or dendrite which protrude into adjacent boutons. The projections are thus surrounded by an invagination of bouton plasmalemma. A distinctive coat occurs at the tip of these bouton invaginations on the cytoplasmic surface of the membrane (see Fig. 10 and Westrum and Blackstad, 1962; Tarrant and Routenberg, 1977). Spinules were located by searching every section in each series for the coated invaginations and included in the analysis only if they were greater in length than width at the narrowest point.

Three-dimensional reconstructions

Electron micrographs were digitized and the images of adjacent sections were microaligned for reconstruction by flickering between the stored image and the live image, and moving the live image to minimize motion of the profiles in the field. The *V8* software from the Children's Hospital Image Graphics Laboratory (IGL) was used to trace the outlines of the synaptic profiles and to compute morphometric data. ICAR software (ISG Technologies, Mississauga, Ontario) was used to display, rotate, and save GIF files of the reconstructed images. Three-dimensional quantities were also computed from the digitized data by using the IGL Trace software developed in the IGL.

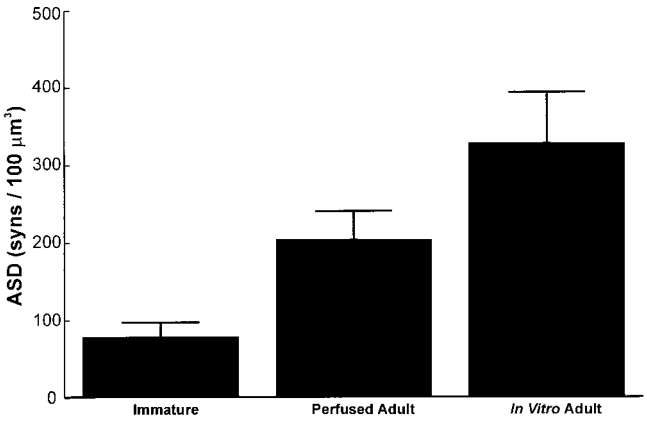

Fig. 3. Incidence of asymmetric synapses (ASD) on spiny dendrites in the immature, adult perfused and adult hippocampal slices maintained in vitro. Adjusted synapse densities (ASD) were calculated using the volume disector and were plotted as the number of synapses per 100 μm^3 of homogeneous neuropil ± S.D. The experimental parameters varied across treatments; hence, a multisample statistical test across all three conditions was inappropriate. A Mann-Whitney test for independent samples revealed the increase in synapse density was significant between the immature (n = 4) and adult perfusion (n = 5) conditions ($P = 0.014$). The contrast between the adult perfused and adult in vitro condition (n = 10) was also statistically significant ($P = 0.005$).

Statistical analysis

Numerical data on synapse densities were analyzed by using Lotus 1-2-3 (Lotus Development Corp., Cambridge MA). Microcal Origin (Microcal Software Inc., Northhampton MA) and Statistica software (StatSoft, Tulsa, OK) were used to graph, obtain means, standard deviations, test for normality, and perform the tests of significance described in the results. The nonparametric Mann-Whitney U test was used to evaluate the significance of differences between samples. In all cases, differences were considered statistically significant when $P < 0.05$.

RESULTS

Prevalence of perforated PSDs increases with maturation

If perforated PSDs are precursors of macular PSDs, as suggested by the splitting hypothesis, then more perforated PSDs would be present during periods of active synaptogenesis (Itarat and Jones, 1993). The relative proportion of macular and perforated synapses was compared in the developing hippocampus during an age of active synaptogenesis (P15) and when total synapse number has reached a plateau (young adults; Steward and Falk, 1991). When viewed through serial sections, macular synapses are continuous PSDs, without holes or gaps, and perforated PSDs are interrupted by electron-lucent regions (Fig. 2). Synapses on nonspiny interneurons were excluded from all analyses because by definition nonspiny cells could not give rise to dendritic spines. Similarly, symmetric, inhibitory synapses do not occur on dendritic spines in hippocampal area CA1 and thus were also excluded from the analyses.

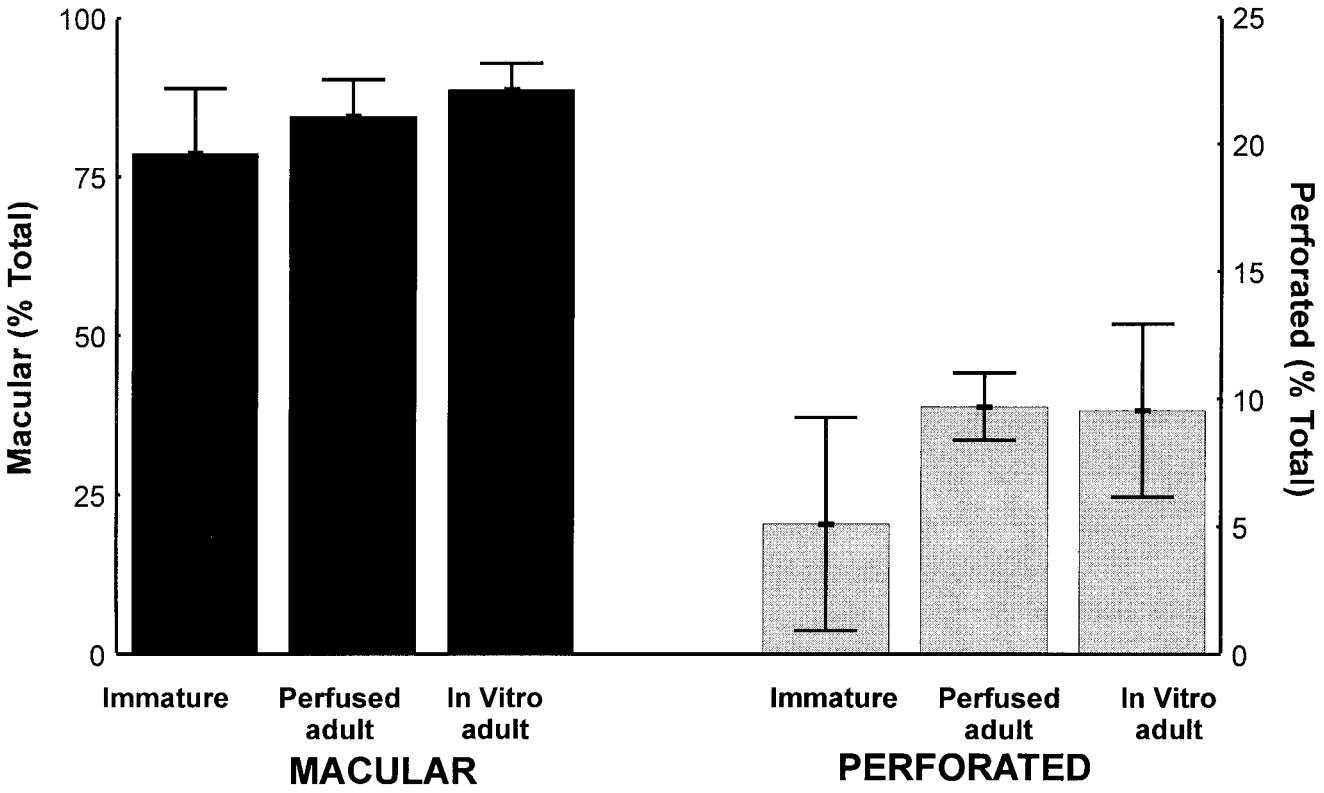

Fig. 4. Relative percentages of macular and perforated synapses in s. radiatum of hippocampal area CA1 of immature, perfused and in vitro adult conditions. The left y-axis is percent macular synapses, and the right y-axis is the percent perforated synapses evaluated on spiny dendrites. Macular synapses predominated in the neuropil across all conditions. A trend existed for a greater proportion of perforated synapses to occupy the adult neuropil, although this failed to reach statistical significance ($P = 0.142$).

Asymmetric macular or perforated synapses occur on a variety of dendritic spine shapes (Fig. 2a–d) as well as on the dendritic shafts of spiny dendrites (Fig. 2e,f). The unbiased analysis by the volume disector revealed an increase in the total number of asymmetric synapses between P15 and adult ages (Fig. 3). Even more synapses occurred in the adult hippocampal slices maintained in vitro, and the significance of this observation is the subject of an ongoing investigation in our laboratory. There were more macular synapses than perforated synapses at both ages (Fig. 4). The greater percentage of perforated PSDs in the adult did not reach statistical significance; however, the trend suggests that perforated PSDs are neither higher during the developing age when synaptogenesis is peaking, nor during the apparent synaptogenesis in adult slices maintained in vitro.

Prevalence of branched spines also increases with maturation

If branched spines were precursors to new daughter spines and resulted from the splitting of previously perforated PSDs, then more branched spines would occur during periods of high synaptogenesis. Dendritic spines were traced to their origins and identified according to Peters and Kaiserman-Abramof (1969) as thin, mushroom, stubby, or branched. Analysis of branched spines using the unbiased volume disector revealed a low relative proportion of branched spines at both ages (Fig. 5). Branched spines were rare, although the increase observed between the immature (P15) and the perfused adult reached statistical significance ($P = 0.05$). Variation in their frequencies is high because some of the samples at both ages did not contain any branched spines.

Diversity in the structure of branched spines

If branched spines arise from the splitting of perforated synapses, then at some point both heads of the branched spines should synapse with the same presynaptic axon. In addition, different heads of a branched spine would be expected to have macular synapses. We evaluated these hypotheses by examining through serial sections the detailed morphology of all the branched spines observed in the P15 and adult series.

Branched dendritic spines share a common origin emerging from a dendrite. Depending on the location of the branch point, the shared origin can have the dimensions of a single spine neck or the added dimensions of the joined spine necks. In Figure 6, a fortuitous section provides a longitudinal view through all of the key components of both branches. One branch is long and thin (Fig. 6,b1), and the other is short and wide (Fig. 6,b2). The two heads of the branched spine are separated by several other dendritic and axonal processes interposed between them. The synapses occur with different axons, which are also separated from one another in the neuropil.

Viewing of serial sections or complete reconstructions were needed to detect and analyze the structure of branched dendritic spines. Eighty-eight adult branched spines were

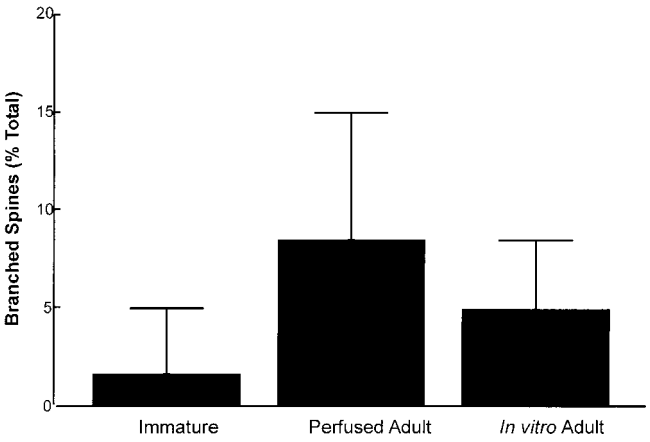

Fig. 5. Relative percentages of branched spines in the neuropil of immature, perfused adult and hippocampal slices maintained in vitro. The branched spines were calculated as the proportion of total spines evaluated from the sampling fields of each condition (mean proportion ± S.D.). The proportion of branched spines ranged from 0% to 6.6% for the postnatal day (P) 15 series (n = 4 series), 2.2–16.5% in the adult perfusion series (n = 5 series), and 0–10.1% in adult hippocampal slices maintained in vitro (n = 10 series).

found in the perfusion-fixed hippocampus and hippocampal slices maintained in vitro (Table 1). Of these, 87 had two branches, 3 had three branches, and 1 had four branches. The heads and necks of all the branched spines were separated by other structures in the neuropil. Most of the adult branched spines had macular PSDs on both heads (Figs. 6, 7, 9, 11a,b). A few of the adult branched spines had perforated synapses on both heads (Figs. 8, 11c), or macular PSDs on one or more heads and a perforated PSD on the other (Fig. 11d). In some cases, one branch was long and thin, whereas the other was a small stubby spine (Figs. 5, 9, and 11b). In other instances, 3 heads of a branched spine all had different morphologies (Fig. 11c). Occasionally, one of the branches had no synapse at all (Fig. 11e). None of these branched spines had microtubules, which contrasts with area CA3, where highly branched dendritic spines occasionally contained microtubules (Chicurel and Harris, 1992).

In the four unbiased samples obtained at P15, there were only two branched spines. For both of these, only one branch had a synapse and no synapse occurred on the other branch (Table 1). A third branched spine was observed in the P15 micrographs, in an adjacent field, on which both heads had macular synapses. All three of the P15 branched spines each had only two branches.

Presynaptic boutons were identified by the number of postsynaptic partners, such that single synapse boutons had one postsynaptic element and multiple synapse boutons had more than one postsynaptic partner. The presynaptic boutons on branched dendritic spines were always widely separated by many dendritic and axonal profiles in the neuropil. The branches of a spine never synapsed with the same bouton (Figs. 6–9; Table 1).

Five reconstructed branched spines were selected to represent the range of morphologies that were detected through serial section viewing (Fig. 11). The dimensions of the individual branches and their associated PSDs varied by more than 10-fold (Table 2), just like individual unbranched dendritic spines in area CA1 (Harris and Stevens,

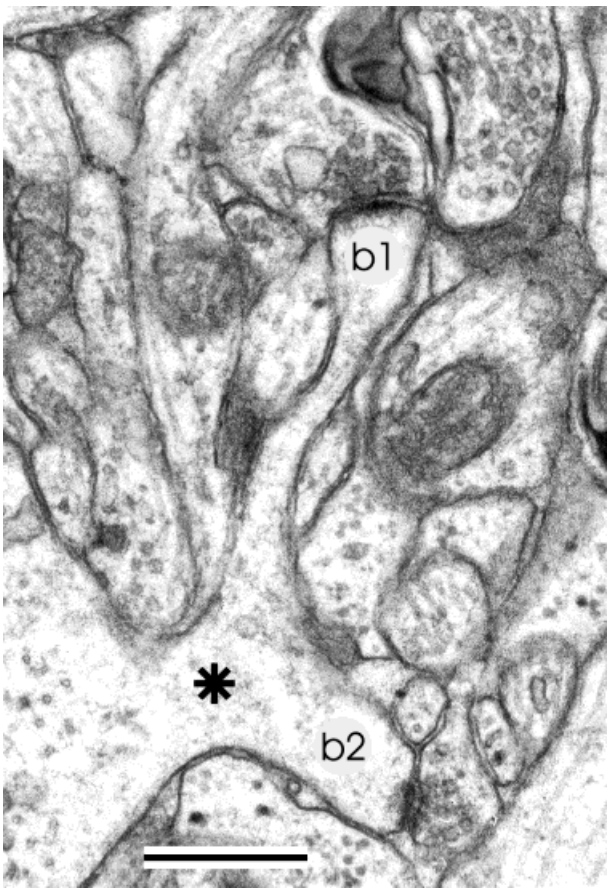

Fig. 6. Fortuitous single section through a branched spine illustrating the shared origin (asterisk) on the parent dendrite and both heads (b1, b2) each of which synapses with a different presynaptic axon. This branched spine was from an adult hippocampal slice maintained in vitro for 4.5 hours. Scale bar = 0.5 μm.

TABLE 1. Synapse Morphologies on Individual Branched Spines in Hippocampal Area CA1

Synaptic characteristics	Adult perfused	Adult in vitro	P15[2] in vivo
All branches had macular PSDs[1]	20	51	1
All branches had perforated PSDs	2	1	—
Both macular and perforated PSDs	4	9	—
Macular PSD on 1 branch, and no synapse on the other branch	1	0	2
Total	27	61	3
Different branches of a single spine synapse with the same presynaptic bouton	0	0	0

[1]PSD, postsynaptic density.
[2]P, postnatal day.

1989; Harris et al., 1992; Sorra and Harris, 1993). The branch point also occurred at highly variable distances from the stalk origin with the parent dendrite.

Synaptic spinules do not divide the presynaptic bouton

If spinules divide the presynaptic axon during splitting, then they should be preferentially located in the perforation of a PSD. Spinules could originate from any part of the spine surface (Figs. 10, 12), and often emerged from the edges of the synapse, in agreement with the findings of

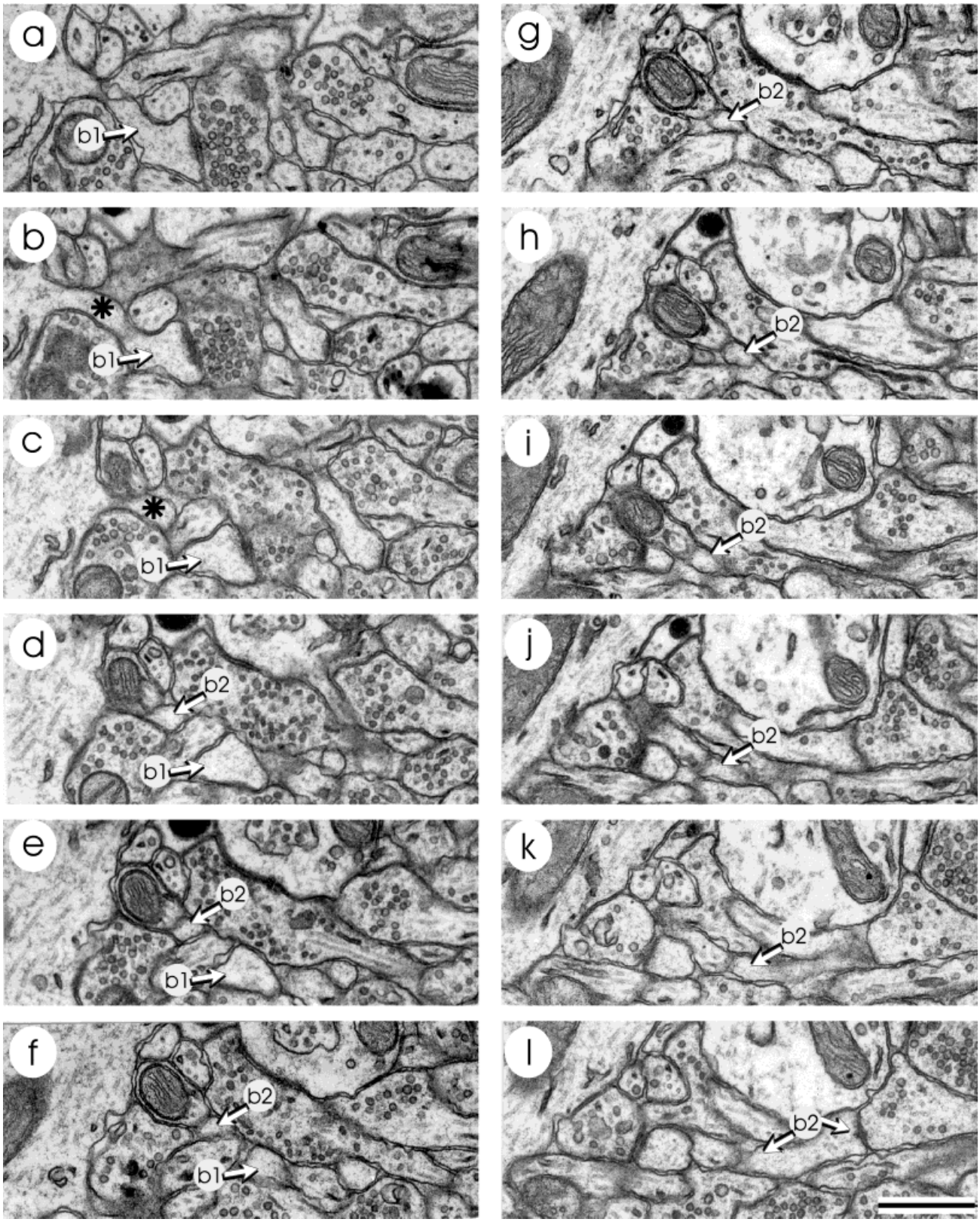

Fig. 7. Set of sequential serial sections (**a–l**) through a branched spine in stratum radiatum of the adult area CA1. The head of branch 1 (b1) is found on sections a through f. The branch point is labeled by an asterisk in b and c, and branch 2 (b2) is found on sections d through l. The individual branches (b1, b2) are separated in the neuropil and synapse with different presynaptic axons. The postsynaptic densities (PSDs) on both b1 and b2 are macular (see sections a–c for b1, and l for b2). These sections were used in the three-dimensional reconstruction displayed in Figure 11a, and were from perfusion-fixed adult hippocampus.

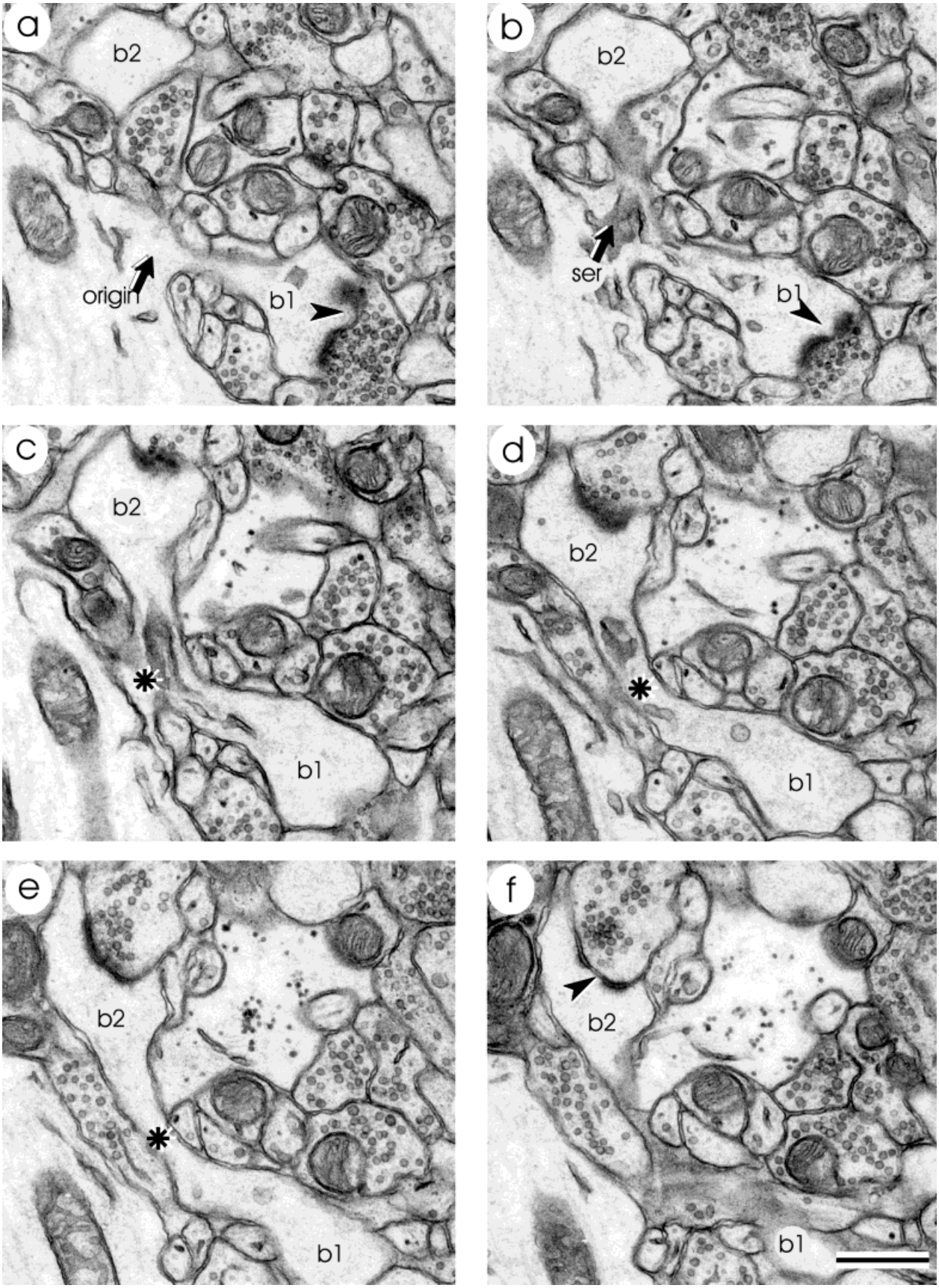

Fig. 8. **a–f:** Sequential serial sections through an adult branched spine in which both synapses are perforated. The origin (origin) with the dendrite occurs on sections a–c. The branch point is clearly visible in sections c through e (asterisk). Smooth endoplasmic reticulum (ser, b) occurs in the branch point and at the base of the spine origin. The postsynaptic density (PSD) on branch 1 (b1) appears perforated in a and b (arrowheads). The perforation in the PSD of branch 2 (b2) is visible in f (arrowhead). Perfusion fixed adult hippocampus. Scale bar = 0.5 μm.

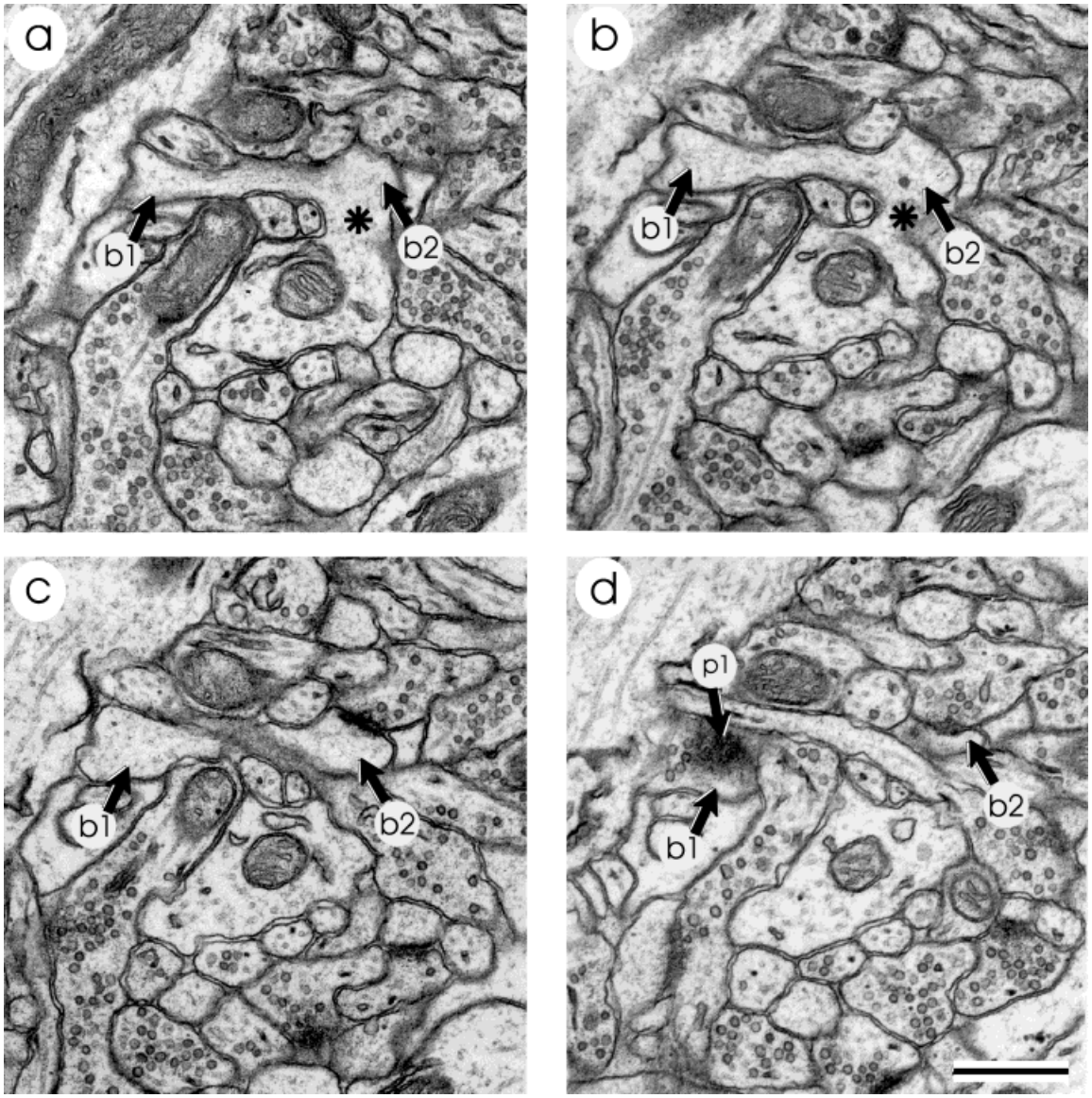

Fig. 9. **a–d:** Sequential serial sections through an adult branched spine where branch 1 (b1) is long and thin and has a macular postsynaptic density (PSD), and branch 2 (b2) is short and stubby, also with a macular PSD. The PSD on the thin branch is sectioned en face in d (p1). Each branch synapses with a different presynaptic bouton. Asterisk, branch origin with dendrite in a and b. Scale bar = 0.5 μm.

Westrum and Blackstad (1962). In all cases, the tip of the spinule was "capped" by a coated pit in the axonal membrane. Thorough examination of 5 EM series (a total volume of 1,220 μm^3) for synaptic spinules revealed 46 occurrences. Table 3 summarizes where these spinules were located. Synaptic spinules most often (52%) originated from the heads of dendritic spines that had macular PSDs (Figs. 10a,b, 12a). These spinules could originate from the edge of the PSD, but never from within the PSD. Spinules occurred less often at perforated synapses (33%) and only 13% of all of the synaptic spinules originated from within the gaps of perforated PSDs (Figs. 10c,d, 12b). In this study, the 6 spinules observed emerging from these gaps did not divide the presynaptic vesicle pool (but see Harris and Sultan, 1995). In some cases (15%), spinules originated from the spine neck (Figs. 10e,f, 12c).

Fig. 10. Ultrastructure of synaptic spinules. **a,b:** Sequential (55 nm) sections of a long spinule (arrows) originating at the edge of a macular synapse. The section of spinule in b connects the pieces in a as seen in the 3-D reconstruction in Figure 12a. **c,d:** Two sections (165 nm apart) through a complex projection at a perforated synapse on the head of a mushroom spine that contains a spine apparatus. In c, one of the spinules projects into the presynaptic axon (white arrow), originating in previous sections from the area of the perforation indicated by the black arrow (reconstructed in Figure 12b, large blue arrow). In d, another projection (white arrow) appears to have emerged from the same perforation in the postsynaptic density (PSD) and is completely surrounded by the presynaptic bouton, thus appearing to be detached from the spine (Fig. 12b, small arrow). **e,f:** Sequential sections of spinules originating from the neck (white arrows) and head (black arrow) of a thin spine with a macular synapse. Both spinules (Fig. 12c, magenta arrows) extend into boutons which are not presynaptic to the spine. Scale bars = 0.5 μm.

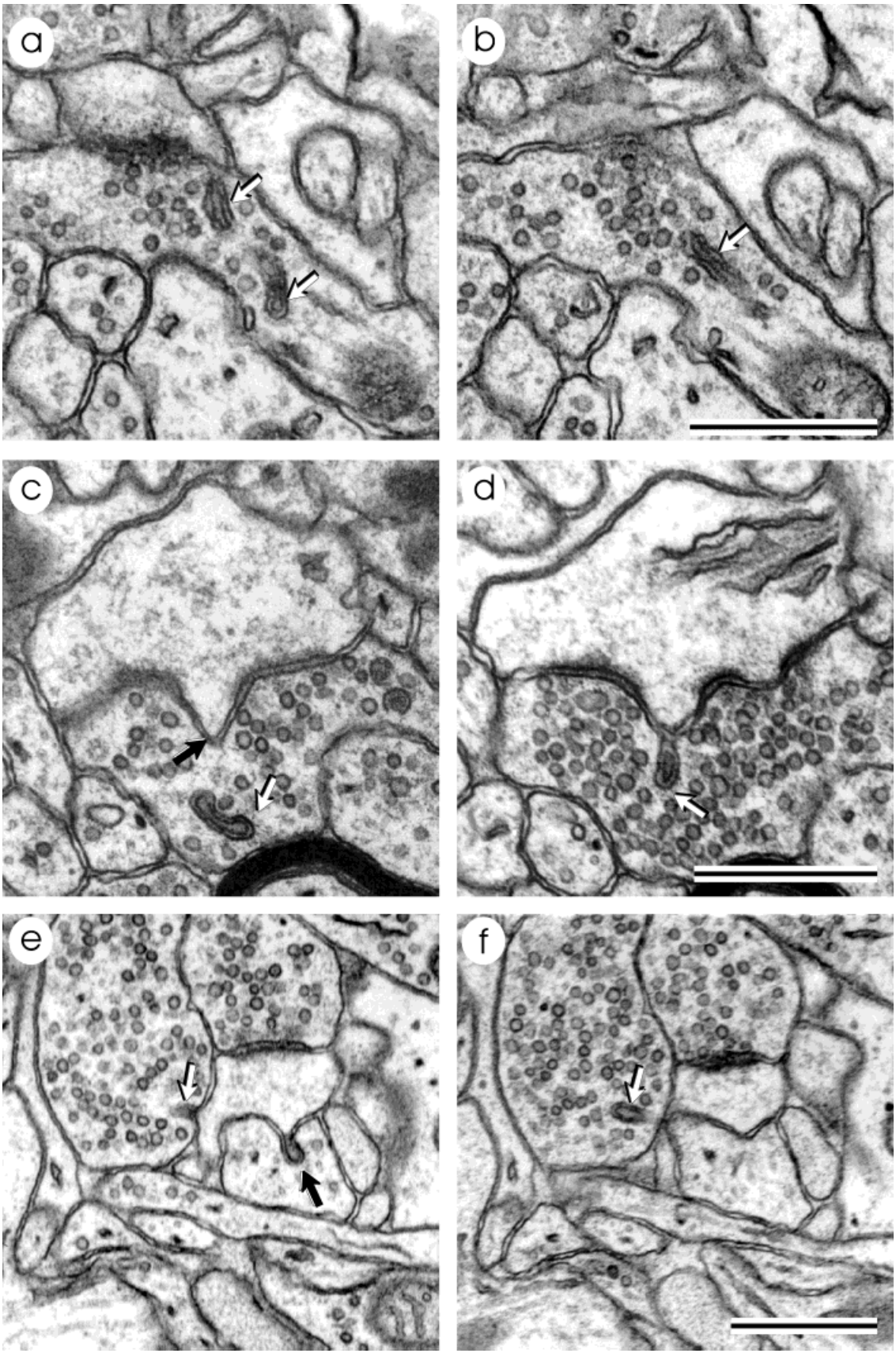

Figure 10

TABLE 2. Dimensions of the Reconstructed Branched Dendritic Spines Illustrated in Figure 11[1]

Figure number	Total volume (μm^3)	Individual branch volumes (μm^3)	Individual PSD[2] areas (μm^2)	Origin to branch length (μm)
11a	0.088	0.038	0.052	0.320
		0.039	0.052	
11b	0.098	0.007	0.023	0.550
		0.075	0.045	
11c	0.225	0.037	0.035	0.420
		0.026	0.043	0.57
		0.144	0.181	
11d	0.421	0.191	0.197	0.080
		0.208	0.320	
11e	0.047	0.024	None	0.250
		0.018	0.050	

[1]The individual branch volumes were computed by graphically removing each branch at the branch points. The top numbers in the columns for individual volumes and PSD area refer to the top leftmost spine branch in each figure; the bottom numbers refer to the bottom rightmost branches. The origin to branch length was computed by tracing from the origin with the parent dendrite through the center of the spine stalk to the branch point, or in the case of 11c to each branch point.
[2]PSD, postsynaptic density.

TABLE 3. Locations of Synaptic Spinules

Description	Quantity
Total number identified	46
Originates from spine head with a macular synapse	24
Originates from spine head with a perforated synapse	9
Originates in the gap of a perforated synapse	6
Originates from the spine neck	7
Extends into a bouton that is not the presynaptic partner	21

Interestingly, a large proportion of the spinules (46%) extended into boutons which were not the presynaptic partners of the spine.

The three reconstructed spines in Figure 12 were selected to illustrate the range in spinule sizes and locations that were observed through serial section viewing. Spines having spinules spanned the full 10-fold range in spine dimensions and the spinules ranged from 0.13 to 0.55 μm in length (Table 4).

TABLE 4. Dimensions of the Spines With Spinules That are Reconstructed in Figure 12

Figure number	Total volume (μm^3)	PSD[1] area (μm^2)	Spinule length (μm)
12a	0.044	0.046	0.55
12b	0.357	0.351	0.43
12c	0.033	0.079	0.17
			0.13

[1]PSD, postsynaptic density.

DISCUSSION

An underlying assumption of structural work has been that differences in form reflect differences in function at the synapse (Harris and Kater, 1994; Shepherd, 1996), like other structures in the biological and physical realm (Thompson, 1942, 1992). It has been possible to identify many different synaptic forms and to examine which morphological processes could be involved in achieving the different forms, but the functional implications remain a topic of intense debate. According to the synapse splitting hypothesis, perforated synapses divide to form independent macular synapses and give rise to new dendritic spines, thereby altering synaptic function. Several lines of evidence argue against this model.

First, perforated synapses increase in parallel with macular ones during maturation, suggesting that perforated PSDs are not necessary precursors of macular PSDs (see also Itarat and Jones 1992, 1993; Jones and Harris, 1995). Second, almost no splitting (i.e., branched) dendritic spines occur at postnatal day 15; thus, synapse splitting is unlikely to be important during development. Third, different parts of a perforated or segmented PSD make synapses with the same presynaptic bouton; therefore, different branches of a splitting dendritic spine should also synapse with the same presynaptic bouton (see also Harris and Stevens, 1989; Harris et al., 1992; Sorra and Harris, 1993, 1998; Harris and Sultan, 1995; Spacek and Harris, 1997). Ninety-one branched dendritic spines were evaluated in the serial EM sections from hippocampal area CA1, the largest sample yet to be analyzed at the ultrastructural level. Different branches of the same spine never synapsed with the same presynaptic bouton. Furthermore, individual spine branch morphologies were as diverse as single spines. Thus, branched spines are unlikely to be transient intermediates in the process of dividing from perforated synapses.

Alternatively, it could be argued that there is a subpopulation of splitting spines not detected because the splitting occurred too rapidly. Such a "rapid" event is unlikely to occur because of the considerable cytoskeletal and membrane rearrangement that would be required. Similarly, it is unlikely that boutons synapsing with different spine branches arose from a single, rapidly splitting bouton. The wide distances between the boutons on different spine heads, and the divergent trajectories of their axons showed that they were not even neighboring boutons splitting along the same axon. Given these constraints, three-dimensional analysis should have detected splitting spines

Fig. 11. Three-dimensional reconstructions of adult branched spines and their synapses. Postsynaptic densities (PSDs) are displayed in red. Reconstructed axonal boutons are only illustrated in a, because they obscure the spine and PSD morphologies in b through e. All spines are graphically removed from their parent dendrites and the origins are on the left side of each reconstruction. a–e are from perfusion-fixed tissue, and b is from a hippocampal slice. **a:** Branched spine with 2 macular synapses on different presynaptic axons. **b:** Spine with one large and one small branch with macular synapses on both branches. **c:** Three branches with a combination of macular and perforated synapses. All branches synapsed with different axons. The blue arrow points to a small spinule in the middle of a perforation. **d:** Spine with 2 branches, and each branch having an annular PSD. An optimal view of one PSD compromised the view of the other (black arrow) due to the 3-D structure of the spine. This spine is similar in shape to the spine illustrated in Figure 7, but is not the same one. **e:** Branched spine with 1 branch with a macular synapse while the other branch has no synapse. Scale bar = 0.5 μm.

Fig. 12. Three-dimensional reconstruction of representative synaptic spinules from adult perfusion-fixed hippocampus area CA1. Postsynaptic densities (PSDs) are displayed in red. **a:** Spinule (blue arrow) originating from the edge of a macular synapse on a thin spine. The spinule is directed into the presynaptic bouton as illustrated in the serial electron micrographs (EMs) of Figure 10a,b. **b:** Spinule (large blue arrow) originating from the periphery of a perforated synapse. A ridge along the perforation projects into the presynaptic bouton between two disconnected PSD segments. A piece of one of these projections (small blue arrow) appears disconnected from the spine (see also Fig. 10c,d). **c:** Spinules (magenta arrows) originating from the neck and head of a spine. These spinules project into boutons which do not make synapses with the spine. Scale bar = 0.5 μm.

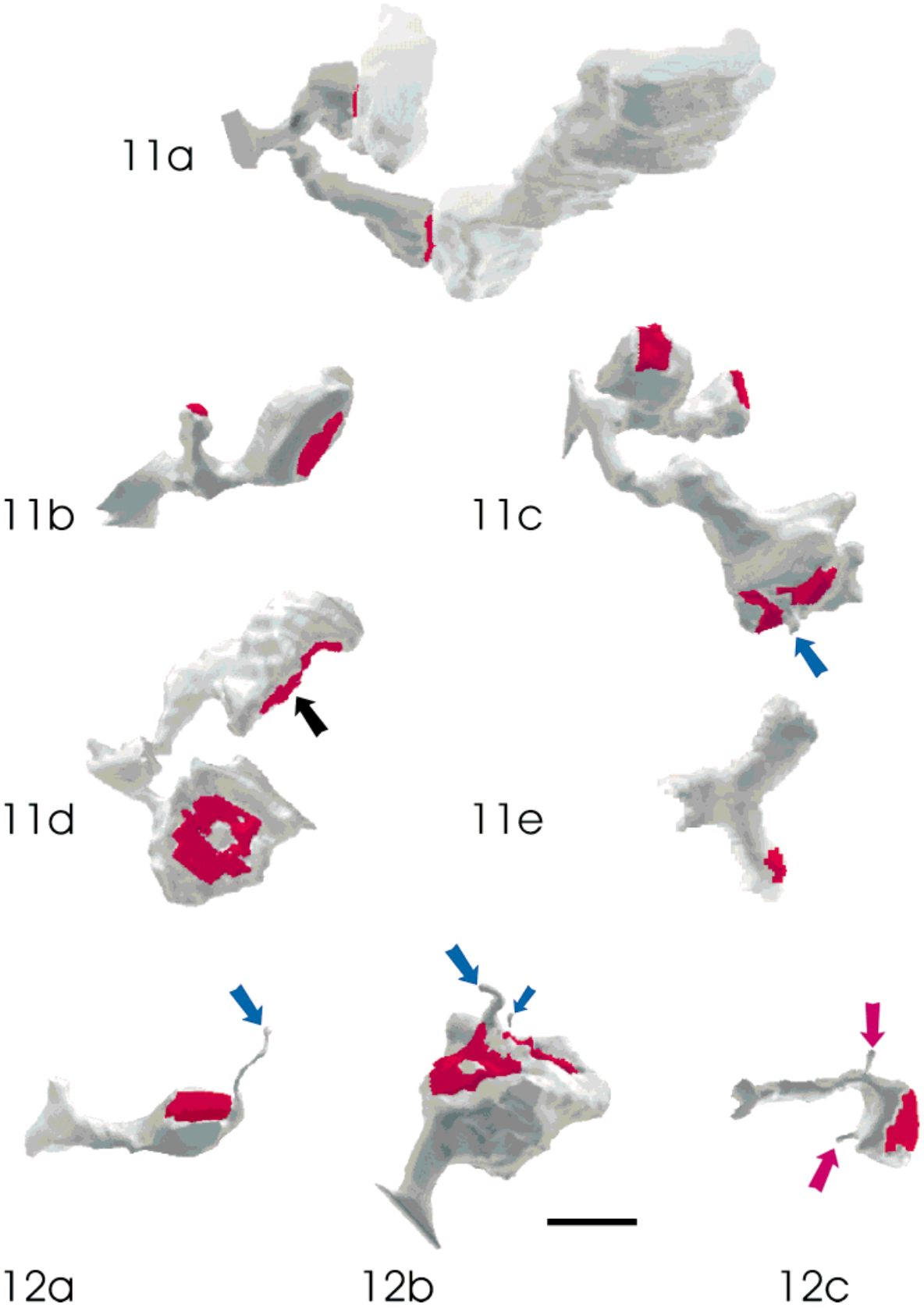

Figures 11 and 12

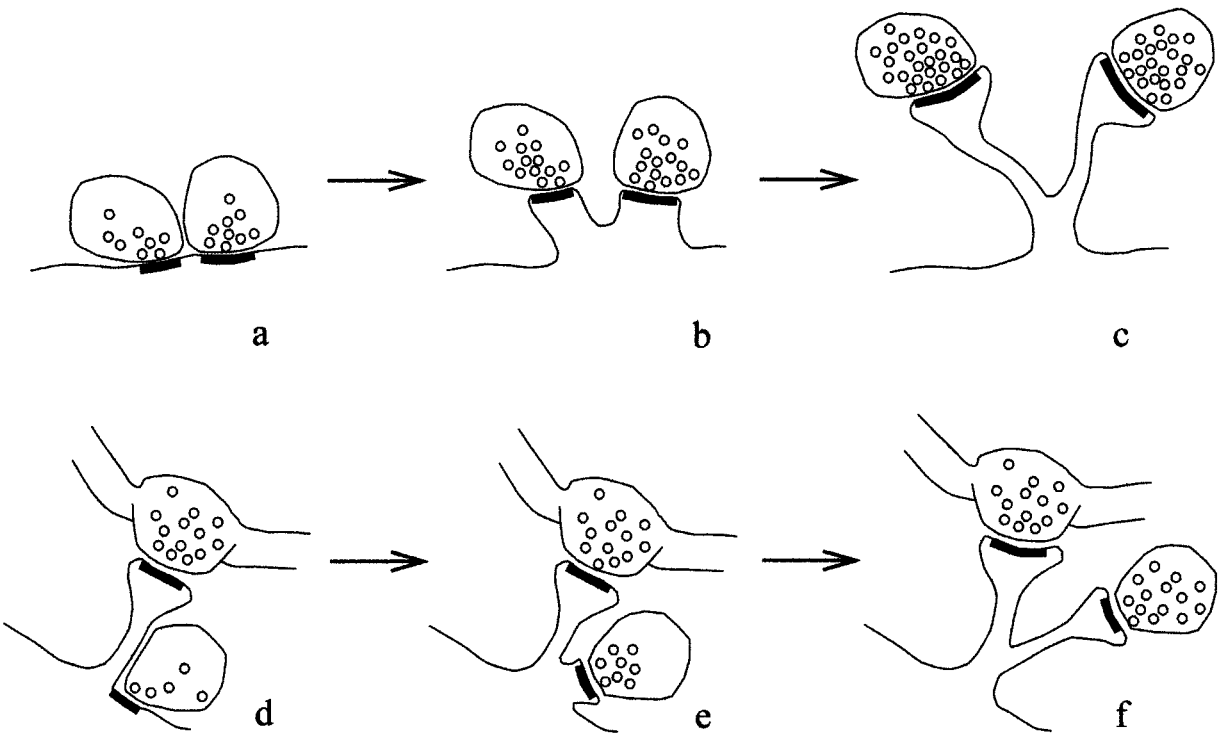

Fig. 13. Diagrammatic model of how branched dendritic spines arise in hippocampal area CA1. **a–c:** Neighboring synapses give rise to branched dendritic spines. **d–f:** A new synapse occurs at the base or on the neck of an existing dendritic spine.

if indeed they were instrumental in the process of new spine formation.

The fourth line of evidence against the synapse splitting hypothesis is that synaptic spinules were too small to divide the axonal boutons into separate presynaptic compartments. In addition, spinules were as likely to emerge from spine necks as from the middle of perforations in the PSD. Furthermore, the spinules often extended into boutons that were not presynaptic to the spine from which the spinule emerged. These data are in agreement with the initial qualitative observations of Westrum and Blackstad (1962) and suggest that the occasional appearance of a spinule in the perforation of a PSD is not indicative of new synapse formation via splitting.

The different branches of branched spines have also been observed to synapse with different axonal boutons in the dentate gyrus (Geinisman et al., 1989; Trommald and Hullenberg, 1997), in cerebellar cortex (Harris and Stevens, 1988), and in neocortex (M. Friedlander personal communication; see also Friedlander et al., 1991). In contrast, the highly branched dendritic spines in hippocampal area CA3 (Chicurel and Harris, 1992) and in the glomeruli of the thalamus (Spacek and Liberman, 1974) have multiple synapses with the same presynaptic bouton. Thus, depending on the brain region, different branches of a single spine synapse preferentially with multiple or with single presynaptic axons, suggesting that division of a presynaptic bouton is not part of synapse splitting to generate new unbranched spines.

The known morphological data suggest that branched spines do not arise from splitting synapses. How then could branched spines arise? During development, most synapses occur directly on the dendritic shaft; hence, it has been suggested that unbranched spines originate directly from these shaft synapses (e.g., Harris et al., 1992; Jones and Harris, 1995). If the initial synapses made by two different presynaptic boutons were to occur close together, the resulting dual spine outgrowth could result in a common origin, giving rise to a branched morphology (Fig. 13a–c). In addition, spine branches could arise from the base or necks of previously unbranched dendritic spines (Fig. 13d–f). This second mechanism is consistent with the (rare) observations of synapses on spine necks or stubby spine branches in area CA1 (see Figs. 8, 11b) and elsewhere in the brain (Spacek and Hartmann, 1983; Horner, 1992).

There is a variation of the synapse-splitting hypothesis that does not require spine splitting (or branching). The PSD is proposed to split while on a spine head and then the spine is thought to retract, leaving a segmented PSD on the dendritic shaft (Carlin and Siekevitz, 1983; Geinisman et al., 1996). Eventually, two new spines emerge, one at each of the PSD segments. Perforated synapses are known to occur directly on the dendritic shaft as early as 19 days gestation in neocortex (Itarat and Jones, 1992, 1993) and postnatal day 7 in hippocampal area CA1 (Harris et al., 1989). Thus, spines with perforated PSDs could also arise directly from the dendritic shaft during development, not needing a cycle of synapse splitting and spine retraction to form.

There is now experimental evidence to support the hypothesis that perforations in PSDs are not permanent features of the synapse, but instead occur transiently in response to synaptic activation (as first proposed by Cohen

and Siekovitz, 1978). Pre- and postsynaptic elements are firmly held together at the site of the synaptic junction by cell-adhesion molecules (Fannon and Colman, 1996; Uchida et al., 1996; Spacek and Harris, 1998). When presynaptic vesicles fuse with the plasma membrane, adhesion molecules in the PSD which span the synaptic cleft would need to slide to the side to accommodate the insertion of vesicular membrane on the presynaptic side. Alternatively, there could be coincidental insertion of smooth vesicles in the postsynaptic spine head to create the perforation (Maletic-Savatic et al., 1995; Spacek and Harris, 1997; Lledo et al., 1998). At large active synapses, vesicular insertion in the middle of the PSD would open a "hole" or perforation in the PSD. At the smaller macular synapses, the PSD molecules would need only to slide to one side of the vesicular release site, leaving the smaller PSD intact. The degree of perforation would depend on the total number of vesicles released over a period of seconds to minutes. This hypothesis is supported by a recent study, wherein massive vesicular release was stimulated in the presence of agents which blocked the recycling of presynaptic vesicles and resulted in the rapid enlargement and perforation of postsynaptic densities (Shupliakov et al., 1997; see also Van Harreveld and Trubatch, 1975; Trubatch et al., 1979; Kadota et al., 1993; Wojtowicz et al., 1994).

The number of synaptic spinules increases just 1 minute after 40-Hz stimulation and thus, these structures could also occur transiently (Applegate and Landfield, 1988). The presence of a coated vesicle on the axonal side of the spinule suggests that they could be involved in endocytosis and engulfment of spine membrane by adjacent axons. For example, if the hypothesis is correct that perforations are transient, then presynaptic engulfment of the postsynaptic membrane would be a rapid way to remove postsynaptic membrane in conjunction with the recycling of presynaptic vesicles. If perforated synapses and spinules come and go with different levels of synaptic activity, then changes in the PSD morphology would be independent of spine branching, which is consistent with the occurrence of perforated PSDs on both branched and unbranched spines. If the synaptic perforations are transient, then their proposed role in long term information storage will need reconsideration.

ACKNOWLEDGMENTS

This work was supported by NIH grants NS21184 and NS33574, and MH/DA57351 which is funded jointly by NIMH, NIDA, NASA (K.M.H.), Mental Retardation Research Center, grant P30-HD18655 (Dr. Joseph Volpe, PI), and Harvard Medical School, and the Natural Sciences and Engineering Research Council of Canada (K.E.S.).

LITERATURE CITED

Aika, Y., J.Q. Ren, K. Kosaka, and T. Kosaka (1994) Quantitative analysis of GABA-like-immunoreactive and parvalbumin-containing neurons in the CA1 region of the rat hippocampus using a stereological method, the disector. Exp. Brain Res. *99:*267–276.

Applegate, M.D., D.S. Kerr, and P.W. Landfield (1987) Redistribution of synaptic vesicles during long-term potentiation in the hippocampus. Brain Res. *401:*401–406.

Applegate, M.D. and P.W. Landfield (1988) Synaptic vesicle redistribution during hippocampal frequency potentiation and depression in young and aged rats. J. Neurosci. *8:*1096–1111.

Bolshakov, V.Y., H. Golan, E.R. Kandel, and S.A. Siegelbaum (1997) Recruitment of new sites of synaptic transmission during the cAMP-dependent late phase of LTP at CA3-CA1 synapses in the hippocampus. Neuron *19:*635–651.

Braendgaard, H. and H.J.G. Gundersen (1986) The impact of recent stereological advances on quantitative studies of the nervous system. J. Neurosci. Methods *18:*39–78.

Carlin, R.K. and P. Siekevitz (1983) Plasticity in the central nervous system: Do synapses divide? Proc. Natl. Acad. Sci. USA *80:*3517–3521.

Chicurel, M.E. and K.M. Harris (1992) Three-dimensional analysis of the structure and composition of CA3 branched dendritic spines and their synaptic relationships with mossy fiber boutons in the rat hippocampus. J. Comp. Neurol. *325:*169–182.

Coggeshall, R.E. and H.A. Lekan (1996) Methods for determining numbers of cells and synapses: A case for more uniform standards of review. J. Comp. Neurol. *364:*6–15.

Cohen, R.S. and P. Siekevitz (1978) Form of the postsynaptic density. A serial section study. J.Cell Biol. *78:*36–46.

Dailey, M.E. and S.J. Smith (1996) The dynamics of dendritic structure in developing hippocampal slices. J. Neurosci. *16:*2983–2994.

Dyson, S.E. and D.G. Jones (1984) Synaptic remodeling during development and maturation: Junction differentiation and splitting as a mechanism for modifying connectivity. Dev. Brain Res. *13:*125–137.

Edwards, F.A. (1995) LTP—a structural model to explain the inconsistencies. Trends Neurosci. *18:*250–255.

Fannon, A.M. and D.R. Colman (1996) A model for central synaptic junctional complex formation based on the differential adhesive specificities of the cadherins. Neuron *17:*423–434.

Friedlander, M.J., K.A. Martin, and D. Wassenhove-McCarthy (1991) Effects of monocular visual deprivation on geniculocortical innervation of area 18 in cat. J. Neurosci. *11:*3268–3288.

Geinisman, Y., F. Morrell, and L. deToledo-Morrell (1989) Perforated synapses on double-headed dendritic spines: A possible structural substrate of synaptic plasticity. Brain Res. *480:*326–329.

Geinisman, Y., L. deToledo-Morrell, F. Morrell, R.E. Heller, M. Rossi, and R.F. Parshall (1993) Structural synaptic correlate of long-term potentiation: Formation of axospinous synapses with multiple, completely partitioned transmission zones. Hippocampus *3:*435–446.

Geinisman, Y., L. deToledo-Morrell, F. Morrell, I.S. Persina, and M.A. Beatty (1996) Synapse restructuring associated with the maintenance phase of hippocampal long-term potentiation. J. Comp. Neurol. *368:*413–423.

Gundersen, H.J. (1978) Estimators of the number of objects per area unbiased by edge effects. Microsc. Acta *81:*107–117.

Harris, K.M. and S.B. Kater (1994) Dendritic spines: Cellular specializations imparting both stability and flexibility to synaptic function. Annu. Rev. Neurosci. *17:*341–371.

Harris, K.M. and J.K. Stevens (1988) Dendritic spines of rat cerebellar Purkinje cells: Serial electron microscopy with reference to their biophysical characteristics. J.Neurosci. *8:*4455–4469.

Harris, K.M. and J.K. Stevens (1989) Dendritic spines of CA1 pyramidal cells in the rat hippocampus: Serial electron microscopy with reference to their biophysical characteristics. J.Neurosci. *9:*2982–2997.

Harris, K.M. and P. Sultan (1995) Variation in number, location, and size of synaptic vesicles provides an anatomical basis for the non-uniform probability of release at hippocampal CA1 synapses. J. Neuropharmacol. *34:*1387–1395.

Harris, K.M., F.E. Jensen, and B. Tsao (1989) Ultrastructure, development, and plasticity of dendritic spine synapses in area CA1 of the rat hippocampus: Extending our vision with serial electron microscopy and three-dimensional analyses. In V. Chan-Palay and C. Kohler (eds): The Hippocampus—New Vistas, Neurology and Neurobiology Volume 52. New York: Alan R. Liss, pp. 33–52.

Harris, K.M., F.E. Jensen, and B. Tsao (1992) Three-dimensional structure of dendritic spines and synapses in rat hippocampus (CA1) at postnatal day 15 and adult ages: Implications for the maturation of synaptic physiology and long-term potentiation. J. Neurosci. *12:*2685–2705.

Horner, C.H. (1993) Plasticity of the dendritic spine. Prog. Neurobiol. *41:*281–321.

Itarat, W. and A. Jones (1992) Perforated synapses are present during synaptogenesis in rat neocortex. Synapse *11:*279–286.

Itarat, W. and D.G. Jones (1993) Morphological characteristics of perforated synapses in the latter stages of synaptogenesis in rat neocortex: Stereological and three-dimensional approaches. J.Neurocytol. *22:*753–764.

Jensen, F.E. and K.M. Harris (1989) Preservation of neuronal ultrastructure in hippocampal slices using rapid microwave-enhanced fixation. J. Neurosci. Methods. *29:*217–230.

Jones, D.J. and R.J. Harris (1995) An analysis of contemporary morphological concepts of synaptic remodelling in the CNS: Perforated synapses revisited. Rev. Neurosci. *6:*177–219.

Jones, T.A., A.Y. Klintsova, V.L. Kilman, A.M. Sirevaag, and W.T. Greenough (1997) Induction of multiple synapses by experience in the visual cortex of adult rats. Neurobiol. Learn. Mem. *68:*13–20.

Kadota, T., M. Mizote, K. Moroi, N. Ozaki, K. Kadota (1993) Rapid recovery of structure and function of the cholinergic synapses in the cat superior cervical ganglion in vivo following stimulation-induced exhaustion. J. Neurocytol. *22:*743–752.

Lledo, P.M., X. Zhang, T.C. Sudhof, R.C. Malenka, and R.A. Nicoll (1998) Postsynaptic membrane fusion and long-term potentiation. Science *279:*399–403.

Maletic-Savatic, M.M., T. Koothan, and R. Malinow (1995) Dendritic calcium-dependent exocytosis in cultured hippocampal neurons: role of calcium/calmodulin protein kinase II. Soc. Neuroscience Abstracts *21:*1743.

Nieto-Sampedro, M., S.F. Hoff, and C.W. Cotman (1982) Perforated postsynaptic densities: Probable intermediates in synapse turnover. Proc. Natl. Acad. Sci. U.S.A. *79:*5718–5722.

Papa, M. and M. Segal (1996) Morphological plasticity in dendritic spines of cultured hippocampal neurons. Neuroscience *71:*1005–1011.

Peters, A. and I.R. Kaiserman-Abramof (1970) The small pyramidal neuron of the rat cerebral cortex. The perikaryon, dendrites and spines. J. Anat. *127:*321–356.

Peters, A., S.L. Palay, and H.d. Webster (1991) The Fine Structure of the Nervous System: The Neurons and Supporting Cells. Philadelphia, London, Toronto: W.B. Saunders, Co.

Robinson, T.E. and B. Kolb (1997) Persistent structural modifications in nucleus accumbens and prefrontal cortex neurons produced by previous experience with amphetamine [In Process Citation]. J. Neurosci. *17:* 8491–8497.

Rusakov, D.A., G. Richter-Levin, M.G. Stewart, and T.V. Bliss (1997) Reduction in spine density associated with long-term potentiation in the dentate gyrus suggests a spine fusion-and-branching model of potentiation [In Process Citation]. Hippocampus. *7:*489–500.

Schuster, T., M. Krug, and J. Wenzel (1990) Spinules in axospinous synapses of the rat dentate gyrus: Changes in density following long-term potentiation. Brain Res. *523:*171–174.

Shepherd, G.M. (1996) The dendritic spine: A multifunctional integrative unit. J.Neurophysiol. *75:*2197–2210.

Shupliakov, O., P. Low, D. Grabs, H. Gad, H. Chen, C. David, K. Takei, C.P. De, and L. Brodin (1997) Synaptic vesicle endocytosis impaired by disruption of dynamin-SH3 domain interactions. Science *276:*259–263.

Sorra, K.E. and K.M. Harris (1993) Occurrence and three-dimensional structure of multiple synapses between individual radiatum axons and their target pyramidal cells in hippocampal area CA1. J. Neurosci. *13:*3736–3748.

Sorra, K.E. and K.M. Harris (1998) Stability in synapse number and size at 2 hr after long-term potentiation in hippocampal area CA1. J. Neurosci. *18:*658–671.

Spacek, J. (1985) Relationships between synaptic junctions, puncta adhaerentia and the spine apparatus at neocortical axo-spinous synapses. Anat. Embryol. *173:*129–135.

Spacek, J. and K.M. Harris (1998) Three-dimensional organization of cell adhesion junctions at synapses and dendritic spines in area CA1 of the rat hippocampus. J. Comp. Neurol. *393:*58–68.

Spacek, J. and K.M. Harris (1997) Three-dimensional organization of smooth endoplasmic reticulum in hippocampal CA1 dendrites and dendritic spines of the immature and mature rat. J. Neurosci. *17:*190–203.

Spacek, J. and M. Hartmann (1983) Three-dimensional analysis of dendritic spines: I. Quantitative observations related to dendritic spine and synaptic morphology in cerebral and cerebellar cortices. Anat. Embryol. *167:*289–310.

Spacek, J. and A.R. Lieberman (1974) Ultrastructure and three-dimensional organization of synaptic glomeruli in rat somatosensory thalamus. J. Anat. (Lond) *117:*487–516.

Steward, O. and P.M. Falk (1991) Selective localization of polyribosomes beneath developing synapses: A quantitative analysis of the relationships between polyribosomes and developing synapses in the hippocampus and dentate gyrus. J. Comp. Neurol. *314:*545–557.

Tarrant, S.B. and A. Routtenberg (1977) The synaptic spinule in the dendritic spine: Electron microscopic study of the hippocampal dentate gyrus. Tissue Cell *9:*461–473.

Thompson, D.W. (1942) On growth and form. The complete revised edition. Republished in 1992. New York, NY: Dover Publications, Inc.

Trommald, M. and G. Hulleberg (1997) Dimensions and density of dendritic spines from rat dentate granule cells based on reconstructions from serial electron micrographs. J. Comp. Neurol. *377:*15–28.

Trommald, M., J.L. Vaaland, T. Blackstad, and P. Andersen (1990) Neurotoxicity of excitatory amino acids. In A. Guidotti and E. Costa (eds): Dendritic Spine Changes in Rat Dentate Granule Cells Associated With Long-Term Potentiation. New York: Raven, pp. 163–174.

Trubatch, J., A. Van Harreveld, A. V. Loud (1979) Change in shape of dendritic spines resulting from KC1 and 4-aminopyridine stimulation of frog brain. In M.A.B. Brazier (ed): Brain Mechanisms in Memory and Learning. Raven Press: New York, p. 37–46.

Uchida, N., Y. Honjo, K.R. Johnson, M.J. Wheelock, and M. Takeichi (1996) The catenin/cadherin adhesion system is localized in synaptic junctions bordering transmitter release zones. J Cell Biol. *135:*767–779.

Van Harreveld A., J. Trubatch (1975) Synaptic changes in frog brain after stimulation with potassium chloride. J. Neurocytol. *4:*33–46.

Westrum, L.E. and T. Blackstad (1962) An electron microscopic study of the stratum radiatum of the rat hippocampus (regio superior, CA1) with particular emphasis on synaptology. J. Comp. Neurol. *119:*281–309.

Wojtowicz, J.M., L. Marin, H.L. Atwood (1994) Activity-induced changes in synaptic release sites at the crayfish neuromuscular junction. J. Neurosci. *14:*3688–3703.

Woolley, C.S., H.J. Wenzel, and P.A. Schwartzkroin (1996) Estradiol increases the frequency of multiple synapse boutons in the hippocampal CA1 region of the adult female rat. J. Comp. Neurol. *373:*108–117.